**Cover**

Computer graphical representation of the tunnelling profile of the metalloprotein Zn7-metlothionein. "Peaks" represent regions of enhanced tunnelling conductance.

Free site-wide access to Advance Articles and the electronic form of this journal is provided with a full-rate institutional subscription.

See www.rsc.org/ejs for more information

contents

FEATURE ARTICLE

393



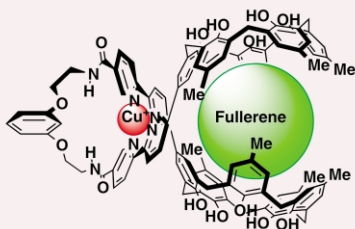
The scanning probe microscopy of metalloproteins and metalloenzymes

Jason J. Davis and H. Allen O. Hill

Tunnelling and single metalloprotein molecules.

COMMUNICATIONS

402

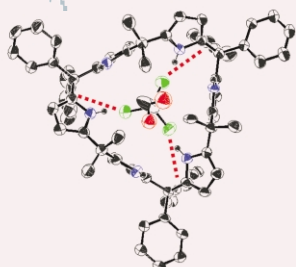


Metal-induced regulation of fullerene complexation with double-calix[5]arene

Takeharu Haino, Yuko Yamanaka, Hiromi Araki and Yoshimasa Fukazawa

The metal-induced regulation of fullerene complexation with double-calix[5]arene is described. The receptor shows strong binding to C₇₀ only in the presence of Cu⁺.

404

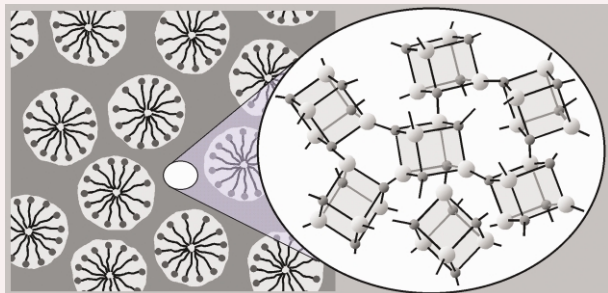


The role of template in the synthesis of *meso*-hexamethyl- *meso*-hexaphenyl-calix[6]pyrrole: trihalogenated compounds as templates for the assembly of a host with a trigonal cavity

Boaz Turner, Alexander Shterenberg, Moshe Kapon, Kinga Suwinska and Yoav Eichen

Trihalogenated compounds act as effective and selective templates in the template-assisted synthesis of *meso*-hexamethyl- *meso*-hexaphenyl-calix[6]pyrrole.

406



Mesoporous aluminophosphates from a single-source precursor

Michael Tiemann and Michael Fröba

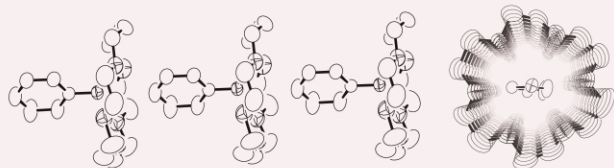
The utilisation of a single-source molecular precursor provides a convenient and rational synthesis route to mesoporous aluminophosphates with a strict ratio of Al:P = 1:1.

408



Formation of a molecular spin ladder induced by a supramolecular cation structure

Sadafumi Nishihara, Tomoyuki Akutagawa, Tatsuo Hasegawa and Takayoshi Nakamura

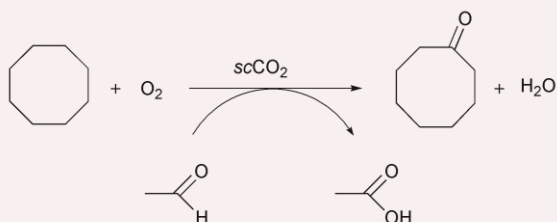


A novel molecular spin ladder structure of $[\text{Ni}(\text{dmit})_2]^-$ ($\text{dmit}^{2-} = 2\text{-thioxo-1,3-dithiole-4,5-dithiolate}$) having $S = 1/2$ spin has been constructed using a supramolecular cation composed of arylammonium and 18-crown-6.

410

Selective oxidation of cyclooctane to cyclooctanone with molecular oxygen in the presence of compressed carbon dioxide

Nils Theyssen and Walter Leitner

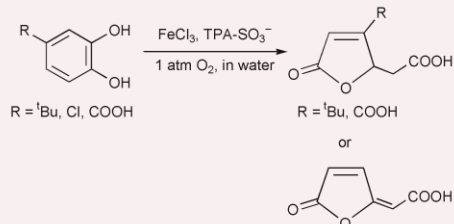


Compressed carbon dioxide provides an excellent inert reaction medium for efficient and selective oxidation of cyclooctane using O_2 -aldehyde mixtures. Up to 20% yields of cyclooctanone were obtained under optimised conditions.

412

Oxygenative cleavage of catechols including protocatechuic acid with molecular oxygen in water catalysed by water-soluble non-heme iron(III) complexes in relevance to catechol dioxygenases

Takuzo Funabiki, Daisuke Sugio, Nobuhiko Inui, Matsutaka Maeda and Yutaka Hitomi

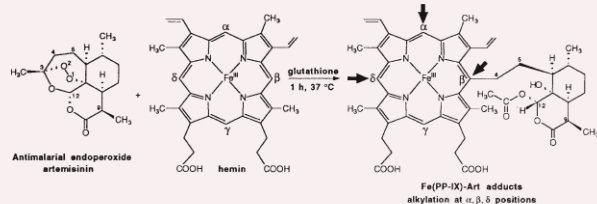


Catechol dioxygenase model oxygenations have been performed for the first time in water by using water-soluble nonheme iron(III) complexes, enabling the oxygenation of protocatechuic acid and other catechols.

414

Alkylation of heme by the antimalarial drug artemisinin

Anne Robert, Yannick Coppel and Bernard Meunier

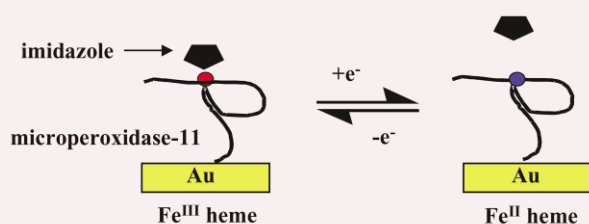


The peroxide function of artemisinin has been activated by iron(II)-heme generated *in situ* from iron(III)-protoporphyrin-IX and glutathione, a biologically relevant reductant. In mild conditions, this reaction produced a high yield (85%) of heme derivatives alkylated at α -, β -, and δ -*meso* positions by a C4-centered radical derived from artemisinin.

416

A model recognition switch. Electrochemical control and transduction of imidazole binding by electrode-immobilized microperoxidase-11

Harold M. Goldston, Jr., Alicia N. Scribner, Scott A. Trammell and Leonard M. Tender



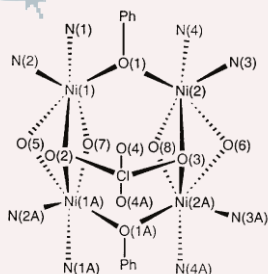
Electrode-immobilized microperoxidase-11 exhibited a titratable potentiometric response to imidazole, demonstrating both molecular recognition and the capability for “switchable” changes in the affinity of an immobilized redox-receptor for a target ligand.

418

A tetranuclear nickel(II) complex assembled from an asymmetric compartmental ligand and bearing an intramolecular [H₃O₂]⁻ bridge

Harry Adams, Scott Clunas and David E. Fenton

The asymmetric di-aminic compartmental proligand HL⁵ on reaction with Ni(ClO₄)₂·6H₂O gives the tetranuclear nickel(II) complex [Ni₄(L⁵)₂(OH)₃(OH₂)ClO₄](PF₆)₂·2CH₃OH·4H₂O in which there is an unusual tetradentate (μ₄,η²)-[H₃O₂]⁻ bridge.

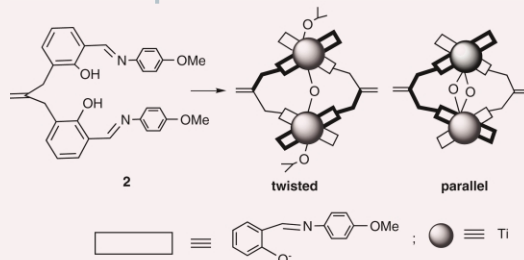


420

Self-assembly of double stranded dinuclear titanium(IV)–Schiff base complexes and formation of intramolecular μ-oxo bridges

Maddali L. N. Rao, Hirohiko Houjou and Kazuhisa Hiratani

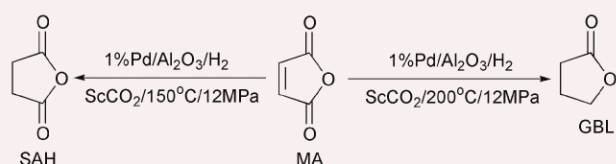
Self assembly of ligand **2** afforded dinuclear titanium complexes with twisted or parallel ligand orientation in the reaction of ligand **2** with titanium isopropoxide



422

Selective hydrogenation of maleic anhydride to γ-butyrolactone over Pd/Al₂O₃ catalyst using supercritical CO₂ as solvent

Unnikrishnan R. Pillai and Endalkachew Sahle-Demessie



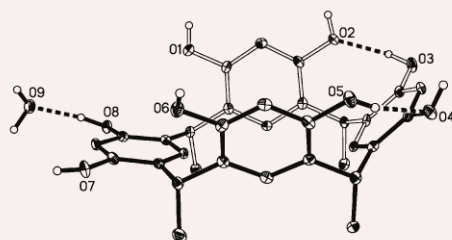
Higher selectivities were achieved for the hydrogenation of maleic anhydride to either γ-butyrolactone or succinic anhydride over simple Pd/Al₂O₃ catalyst using Sc-CO₂ reaction medium than the reaction in organic solvents or under gas phase conditions.

424

A novel scoop-shaped conformation of C-methylcalix[4]resorcinarene in a bilayer structure

Bao-Qing Ma and Philip Coppens

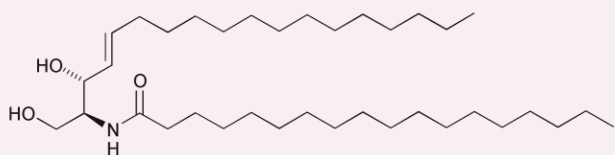
A new scoop-shaped conformation of C-methylcalix[4]resorcinarene has been identified; it is a hybrid of the previously observed crown- and flattened cone conformations.



426

Synthesis of *D*-erythro-sphingosine and *D*-erythro-ceramide

Jacqueline E. Milne, Krzysztof Jarowicki, Philip J. Kocienski and Jorge Alonso

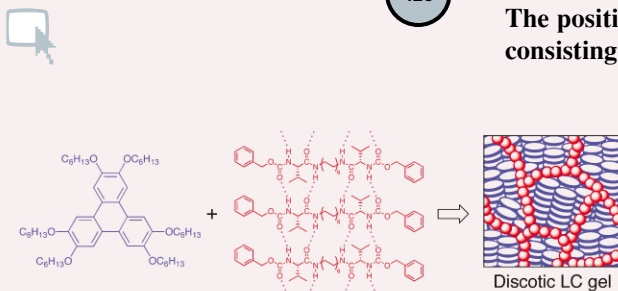


Key features in a synthesis of ceramide and *D*-erythro-sphingosine are (a) the first Cu(I)-mediated 1,2-metallate rearrangement of a glycal derivative; (b) a convenient and tin-free synthesis of α -lithiated glycals by phenylsulfinyl–lithium exchange and (c) an unusual O–C–O silicon shuttle.

428

The positive effect on hole transport behaviour in anisotropic gels consisting of discotic liquid crystals and hydrogen-bonded fibres

Norihiro Mizoshita, Hirosato Monobe, Masaaki Inoue, Masakatsu Ukon, Tsuyoshi Watanabe, Yo Shimizu, Kenji Hanabusa and Takashi Kato

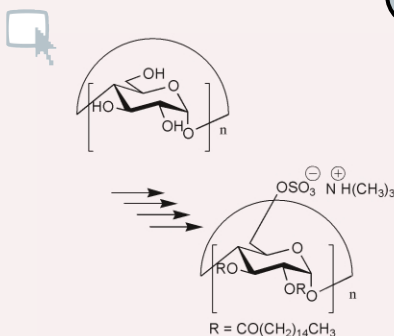


The enhancement of hole mobilities by the introduction of microphase-separated structures has been achieved in discotic liquid-crystalline physical gels.

430

Erythrocyte-like liposomes prepared by means of amphiphilic cyclodextrin sulfates

Takeshi Sukegawa, Tetsuya Furuike, Kenichi Niikura, Akihiko Yamagishi, Kenji Monde and Shin-Ichiro Nishimura

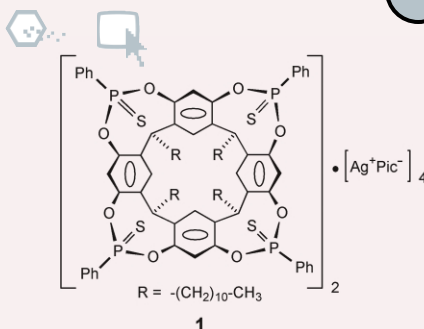


Novel amphiphilic CD sulfates having excellent capacity to form stable monolayers at the air–water interface and interesting erythrocyte-like liposomes were designed.

432

A new supramolecular assembly obtained from the combination of silver(I) cations with a thiophosphorylated cavitaand

Brigitte Bibal, Bernard Tinant, Jean-Paul Declercq and Jean-Pierre Dutasta

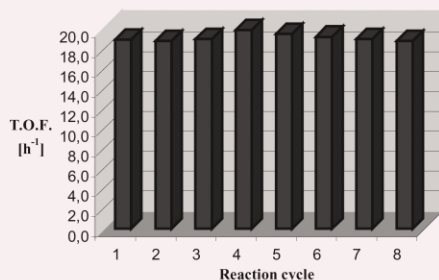


A new structural motif for self-assembly of cavitaands was obtained by coordination of silver(I) cations to thio-phosphorylated cavitaands **1**. This was possible owing to the stereoselective synthesis of the *iiii* isomer of **1**.

434

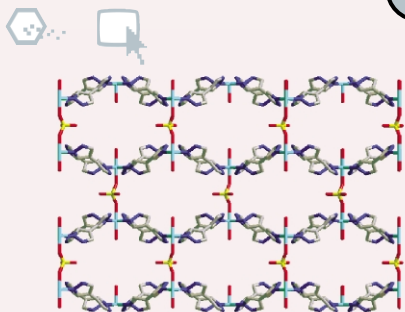
Metal catalysed Michael additions in ionic liquids

Maria Michela Dell'Anna, Vito Gallo, Piero Mastrorilli, Cosimo Francesco Nobile, Giuseppe Romanazzi and Gian Paolo Suranna



The first example of Michael addition reaction in ionic liquids is described. Using Ni(acac)₂ as catalyst high activity, easy product separation and recyclability of the catalytic system was achieved.

436

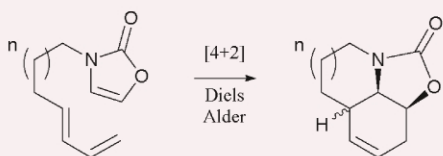


Mixed-anion complexes with a bipyrazolyl ligand. A new entry to a realm of three-dimensional five-connected coordination topologies

Vira V. Ponomarova, Vasiliy V. Komarchuk, Ishtvan Boldog, Alexander N. Chernega, Joachim Sieler and Konstantin V. Domasevitch

Cross-linking of corrugated square grid coordination layers by anionic bridging groups generates 3D five-connected coordination networks.

438

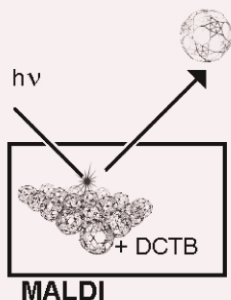


Intramolecular Diels–Alder reactions of N-substituted oxazolones

Stephen Philip Fearnley and Eleonora Market

The first intramolecular Diels–Alder reactions of simple trienes featuring an N-substituted oxazolone as the dienophilic component have been investigated and are reported herein.

440

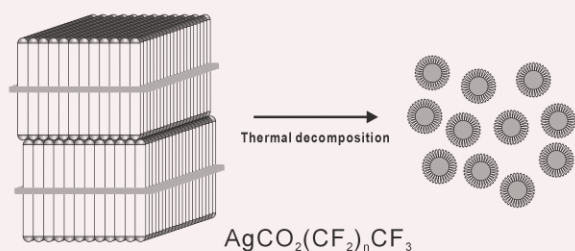


Soccer-playing metal oxide giant spheres: a first step towards patterning structurally well defined nano-object collectives

Achim Müller, Ekkehard Diemann, S. Qaiser Nazir Shah, Christoph Kuhlmann and Matthias C. Letzel

In context with the challenge to assemble giant molecules into patterns with limited size, molybdenum oxide giant spheres (with a molecular mass of about 16 kDa) could be ‘kicked out’ like soccer balls into the gas phase using MALDI and detected by TOF mass spectrometry while cluster collectives ranging from dimers to pentamers were observed.

442

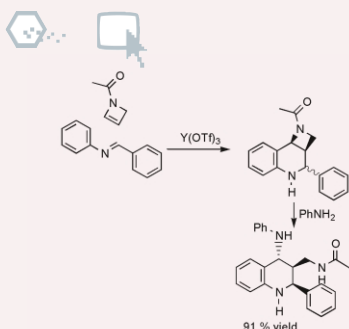


Perfluorocarbon-stabilized silver nanoparticles manufactured from layered silver carboxylates

Seung Joon Lee, Sang Woo Han and Kwan Kim

Perfluorocarboxylate-stabilized silver nanoparticles have been prepared uniformly *via* the thermal decomposition of layered silver perfluorocarboxylates ($\text{AgCO}_2(\text{CF}_2)_n\text{CF}_3$, $n = 10, 12, 14$ and 16).

444

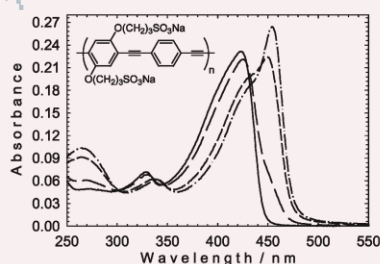


Three component coupling reactions of N-acetyl-2-azetine—rapid stereoselective entry to 2,3,4-trisubstituted tetrahydroquinolines

Paul J. Stevenson, Mark Nieuwenhuyzen and Daire Osborne

N-Acetyl-2-azetine, imines derived from aromatic amine and aromatic primary amine react at room temperature in acetonitrile containing 3 mol% yttrium triflate to give 2,3,4-trisubstituted tetrahydroquinolines in high yield.

446

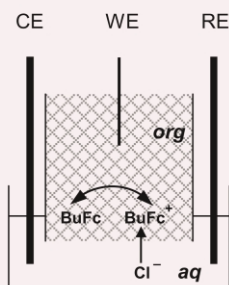


Photophysics, aggregation and amplified quenching of a water-soluble poly(phenylene ethynylene)

Chunyan Tan, Mauricio R. Pinto and Kirk S. Schanze

The fluorescence, absorption and fluorescence quenching properties of an anionic poly(phenylene ethynylene) are investigated in H₂O and methanol solutions.

448

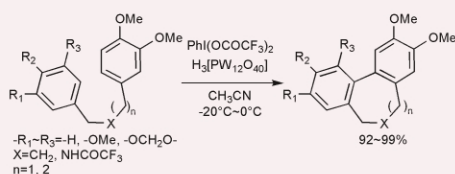


Carbon ceramic electrode modified with redox liquid

Marcin Opallo and Monika Saczek-Maj

A new approach in electrode modification is presented. A hydrophobic liquid redox active modifier (butylferrocene) is introduced into a hydrophobic silicate matrix containing graphite particles.

450



A novel and efficient oxidative biaryl coupling reaction of phenol ether derivatives using a combination of hypervalent iodine(III) reagent and heteropoly acid

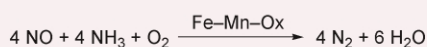
Hiromi Hamamoto, Gopinathan Anilkumar, Hirofumi Tohma and Yasuyuki Kita

A novel and efficient oxidative biaryl coupling reaction of phenol ether derivatives using a combination of hypervalent iodine(III) reagent, phenyliodine(III) bis(trifluoroacetate) (PIFA), and heteropoly acid has been developed.

452

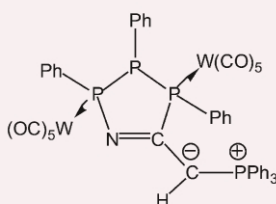
Low temperature selective catalytic reduction (SCR) of NO with NH₃ over Fe–Mn based catalysts

Richard Q. Long, Ralph T. Yang and Ramsay Chang



Fe–Mn based transition metal oxides (Fe–Mn, Fe–Mn–Zr and Fe–Mn–Ti) show nearly 100% NO conversion at 100–180 °C for selective catalytic reduction of NO with NH₃ under the applied conditions with a space velocity of 15 000 h⁻¹.

454



Synthesis of the first 1,2,3,4-azatriphospholene complex

Nils Hoffmann, Cathleen Wismach, Peter G. Jones, Rainer Streubel, Ngoc Hoa Tran Huy and François Mathey

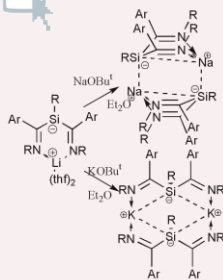
Synthesis of the first 1,2,3,4-azatriphospholene complex was achieved by heating a solution of a *P*-phenyl-substituted 7-phosphanorbornadiene tungsten complex and triphenylphosphonio cyanomethylide.

456

Sodium and potassium 3-sila- β -diketiminates show new coordination modes

James D. Farwell, Peter B. Hitchcock and Michael F. Lappert

The reaction between the lithium 3-sila- β -diketimate (**1**) and the appropriate MOBu⁺ yielded the crystalline sodium (**2**) or potassium (**3**) 3-sila- β -diketimate in high yield.

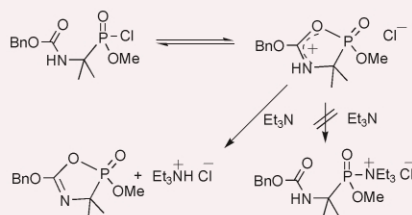


458

Reactive species formed from *N*-benzyloxycarbonyl α -aminophosphonochloridates and triethylamine: probable identity and implications for synthesis

Paul M. Cullis and Martin J. P. Harger

The synthetically useful phosphorylating species formed when a *N*-benzyloxycarbonyl α -aminophosphonochloridate reacts with Et₃N is not a phosphonylammonium salt; spectroscopic evidence points instead to an oxazaphospholine oxide.

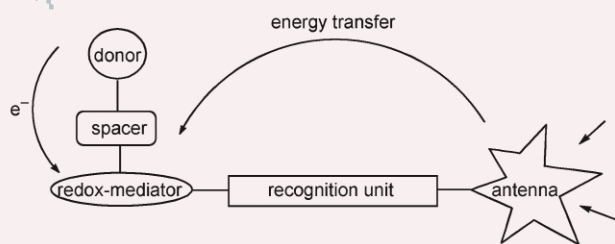


460

Mimicking dye-based functions of natural blue-light photoreceptors by studying photoinduced energy and electron transfer in a pyrene–isoalloxazine(flavin)–phenothiazine triad

Zhen Shen, Joerg Strauss and Joerg Daub

An artificial system containing phenothiazine as electron donor, isoalloxazine as flavinoid redox-mediator and pyrene as antenna has been built up in order to model photoinduced energy and electron transfer processes of natural blue-light photoreceptors.

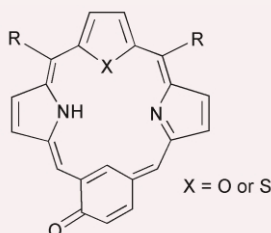


462

Core modified oxybenzoporphyrins: new aromatic ligands for metal–carbon bond activation

Sundararaman Venkatraman, Venkataramanarao G. Anand, Simi K. Pushpan, Jeyaraman Sankar and Tavarekere K. Chandrashekar

Syntheses of two new core modified oxybenzoporphyrins and a neutral palladium complex of oxa-substituted oxybenzoporphyrin is reported.

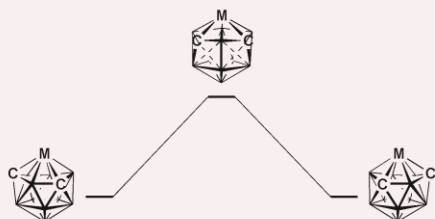


464

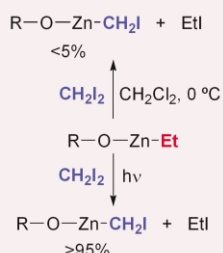
The first supraicosahedral p-block metallocarboranes

Neil M. M. Wilson, David Ellis, Alan S. F. Boyd, Barry T. Giles, Stuart A. Macgregor, Georgina M. Rosair and Alan J. Welch

4,1,6-*closo*-SnC₂B₁₀H₁₂ and 1,6-Me₂-4,1,6-*closo*-SnC₂B₁₀H₁₀ are the first examples of supraicosahedral metallocarboranes containing p-block metals. The former is fluxional in solution, switching between enantiomeric forms *via* a double diamond–square–diamond process with a calculated activation energy of 25.4 kJ mol⁻¹.



466

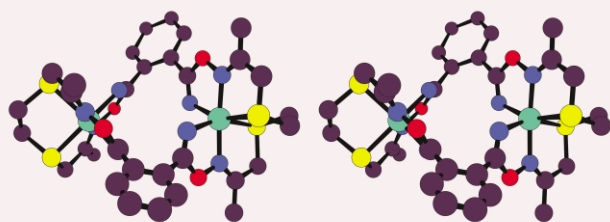


Photoinduced alkyl group exchange of ethylzinc alkoxides: X-ray crystal structure of an iodomethylzinc methoxide

André Charette, André Beauchemin, Sébastien Francoeur, Francine Bélanger-Gariépy and Gary D. Enright

Irradiation of a solution of ethyl zinc alkoxides and CH_2I_2 leads to clean formation of iodomethylzinc alkoxides. The solid-state structure of $(\text{MeO})_8\text{Zn}_7(\text{CH}_2\text{I})_6$ is also reported.

468

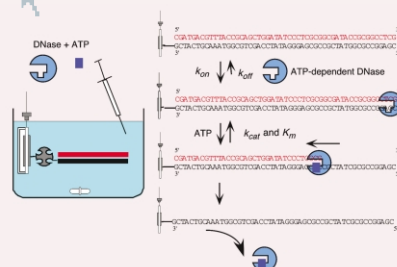


A new class of macrocyclic complexes formed *via* nickel-promoted macrocyclisation of dioxime with dinitrile

Vitaly V. Pavlishchuk, Sergey V. Kolotilov, Anthony W. Addison, Michael J. Prushan, Raymond J. Butcher and Laurence K. Thompson

Nickel(II) promotes coupling of dioxime with dinitrile, to yield the first example of a new class of macrocyclic ligands, the stereoelectronic demands of *o*-phthalonitrile here yielding a dinickel macrocycle.

470

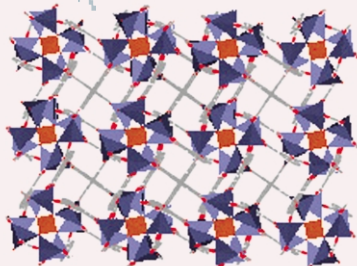


Direct monitoring of DNA cleavages catalyzed by an ATP-dependent deoxyribonuclease on a 27 MHz quartz-crystal microbalance

Hisao Matsuno, Hiroyuki Furusawa and Yoshio Okahata

Each step of DNA degradation by an ATP-dependent DNase could be quantified on one 27 MHz QCM device: binding of the enzyme onto DNA, hydrolysis of DNA, and release of the enzyme from the hydrolyzed DNA.

472

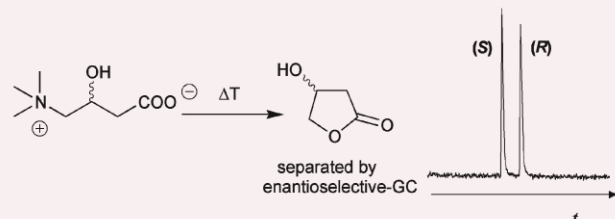
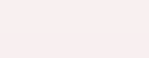


$[\text{Zn}_8(\text{SiO}_4)(\text{C}_8\text{H}_4\text{O}_4)_6]_n$: the firstborn of a metallosilicate–organic hybrid material family ($\text{C}_8\text{H}_4\text{O}_4$ = isophthalate)

S. Y. Yang, L. S. Long, R. B. Huang and L. S. Zheng

The first metallosilicate–organic hybrid material is constructed from $\text{Zn}_8(\text{SiO}_4)$ cores and isophthalate linkers; its diamondoid framework remains stable up to 500°C .

474



The first gas chromatographic resolution of carnitine enantiomers

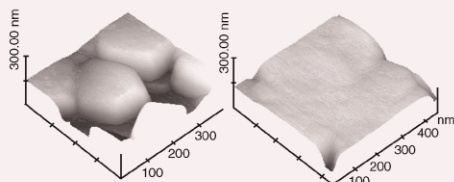
Alessandra Di Tullio, Ilaria D'Acquarica, Francesco Gasparrini, Paola Desiderio, Fabio Giannesi, Sandra Muck, Fabrizio Piccirilli, Maria Ornella Tinti and Claudio Villani

Polar, zwitterionic carnitine enantiomers are resolved by GC on a β -cyclodextrin chiral stationary phase after on-line thermal cyclization to the corresponding β -hydroxy- γ -butyrolactones.

476

Light-assisted chemical deposition of highly (0001) oriented zinc oxide film

Masanobu Izaki

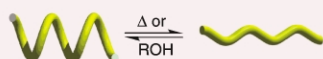
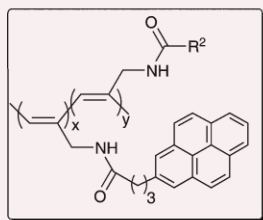


Highly (0001) oriented zinc oxide (ZnO) films of smooth layer type and hexagonal columns have been prepared on quartz glass substrates at temperatures as low as 323 K by UV light assisted chemical deposition from an aqueous solution containing hydrated zinc nitrate and dimethylamine–borane (DMAB).

478

A chromophore-labeled poly(*N*-propargylamide): a new strategy for a stimuli-responsive conjugated polymer

Ryoji Nomura, Katsuhiko Yamada and Toshio Masuda

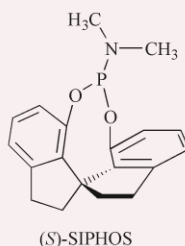


A new stimuli-responsive conjugated polymer was synthesized, where, following the conformational change from helical to disordered state, the fluorescence property of the side chain chromophore changes upon sensing external stimuli.

480

Novel monodentate spiro phosphorus ligands for rhodium-catalyzed hydrogenation reactions

Yu Fu, Jian-Hua Xie, Ai-Guo Hu, Hai Zhou, Li-Xin Wang and Qi-Lin Zhou

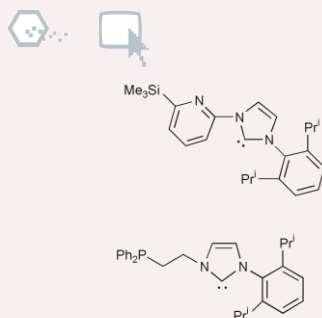


The first monodentate phosphorus ligands containing the spiro structure (SIPHOS) have been synthesized and applied in the asymmetric rhodium-catalyzed hydrogenation of functionalized olefins, providing excellent enantioselectivities (up to 99.3% ee).

482

Synthesis and structural characterisation of stable pyridine- and phosphine-functionalised *N*-heterocyclic carbenes

Andreas A. Danopoulos, Scott Winston, Thomas Gelbrich, Michael B. Hursthouse and Robert P. Tooze

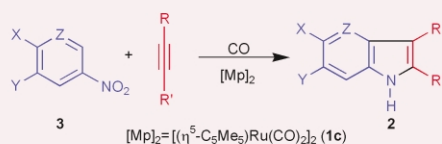


Stable, uncoordinated { 1-[2-(6-trimethylsilyl)pyridyl]-3-[(2,6-diisopropyl)phenyl]imidazol-2-ylidene }, **I**, and { 1-[β-(diphenylphosphino)ethyl]-3-[(2,6-diisopropyl)phenyl]imidazol-2-ylidene }, **II**, have been synthesised; in the solid state they adopt a conformation with the lone pairs in a mutually *anti* arrangement.

484

A novel and direct synthesis of indoles *via* catalytic reductive annulation of nitroaromatics with alkynes

Andrea Penoni and Kenneth M. Nicholas

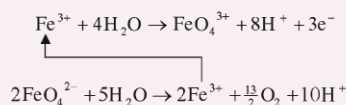


Indoles are produced regioselectively and in moderate yields from the [CpM(CO)₂]₂-catalyzed reactions of nitroaromatics with alkynes under carbon monoxide.

486

Electrochemical generation of ferrate in acidic media at boron-doped diamond electrodes

Joowook Lee, Donald A. Tryk, Akira Fujishima and Su-Moon Park

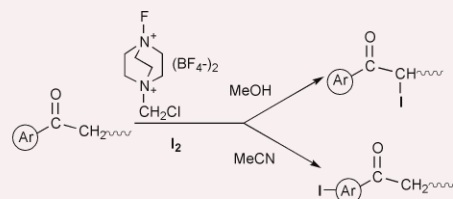


Ferrate(VI) was generated for the first time in acidic media using boron-doped diamond electrodes. The electrochemically generated ferrate(VI) undergoes a rapid degradation reaction with water to reduce back to Fe(III).

488

Selectfluor™ F-TEDA-BF₄ mediated and solvent directed iodination of aryl alkyl ketones using elemental iodine

Stojan Stavber, Marjan Jereb and Marko Zupan

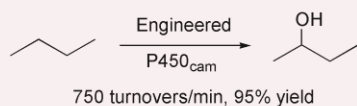


Reactions of aryl alkyl ketones with methanol solution of elemental iodine and 1-fluoro-4-chloromethyl-1,4-diazoniabicyclo[2.2.2]octane bis(tetrafluoroborate) (*Selectfluor*™ F-TEDA-BF₄) result in the formation of corresponding α -iodo ketones.

490

Butane and propane oxidation by engineered cytochrome P450_{cam}

Stephen G. Bell, Julie-Anne Stevenson, Helen D. Boyd, Sophie Campbell, Austin D. Riddle, Erica L. Orton and Luet-Lok Wong

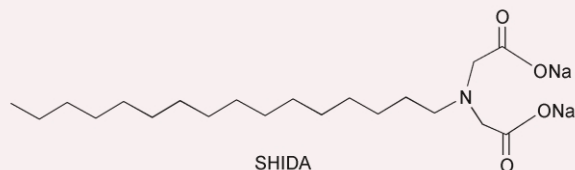


Amino acid substitutions designed to decrease the volume of the cytochrome P450_{cam} substrate pocket dramatically promoted catalytic oxidation of butane and propane to the alcohols, with no further oxidation.

492

Vesicle formation induced by metal ions from micelle-forming sodium hexadecylimino diacetate in dilute aqueous solution

Xuzhong Luo, Sanxie Wu and Yingqiu Liang

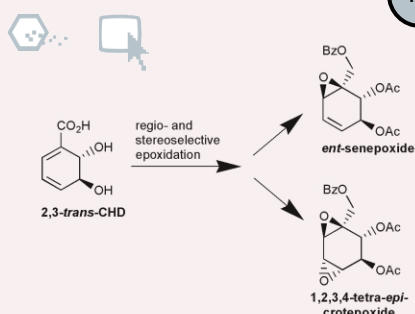


In dilute aqueous solution, micelle-forming sodium hexadecylimino diacetate assembles into vesicles induced by Cu(II), Co(II) and Ni(II) ions.

494

Cyclohexadiene-*trans*-diols as versatile starting material in natural product synthesis: short and efficient synthesis of *iso*-crotepoide and *ent*-senepoxide

Volker Lorbach, Dirk Franke, Martin Nieger and Michael Müller

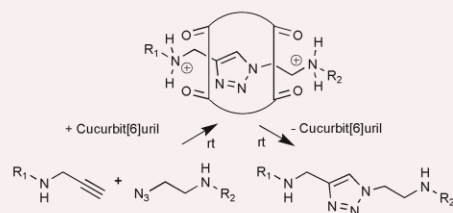


Microbially produced (2*S*,3*S*)-*trans*-dihydroxy-2,3-dihydrobenzoic acid (2,3-*trans*-CHD) is used as starting material in bioactive substance chemistry for the first time. A short and efficient synthesis of *ent*-senepoxide and *iso*-crotoepoxide via regio- and stereoselective epoxidation is described.

496

The synthesis of [2], [3] and [4]rotaxanes and semirotaxanes

Dönüs Tuncel and Joachim H. G. Steinke

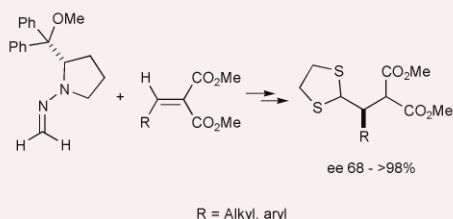


The cucurbituril-catalysed synthesis of [2], [3] and [4]semirotaxanes allows access to regioselectively pure, 1,3-disubstituted mono-, bis- and tris-triazoles in high yield after dethreading.

498

Asymmetric Michael addition of formaldehyde *N,N*-dialkylhydrazones to alkylidene malonates

Juan Vázquez, Auxiliadora Prieto, Rosario Fernández, Dieter Enders and José M. Lassaletta

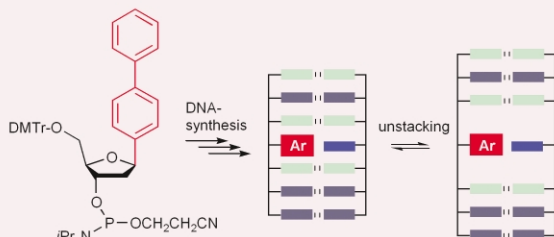


Formaldehyde *N,N*-dialkylhydrazones smoothly add to alkylidene malonates in the presence of MgI_2 . Ensuing racemization-free $BF_3 \cdot OEt_2$ -catalyzed thiolytic cleavage of the hydrazone C=N bond affords the corresponding dithioketals in optically enriched form.

500

Local disruption of DNA-base stacking by bulky base surrogates

Ishwar Singh, Walburga Hecker, Ashok K. Prasad, Virinder S. Parmar and Oliver Seitz

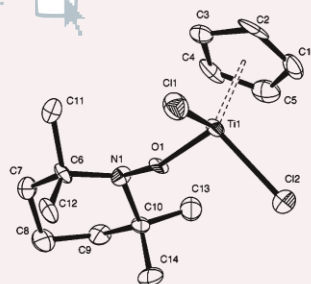


A novel biphenyl base surrogate disrupts 2-aminopurine base stacking while maintaining duplex integrity.

502

Synthesis and molecular structure of titanium complexes containing a reduced TEMPO radical

Mahesh K. Mahanthappa, Kuo-Wei Huang, Adam P. Cole and Robert M. Waymouth

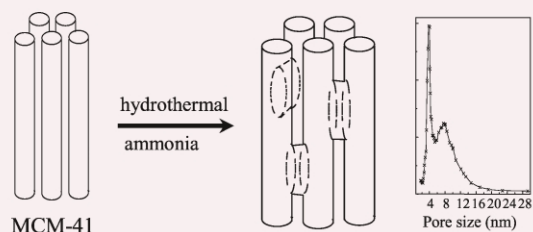


The first structural characterization of titanium complexes containing the monoanionic ligand derived from TEMPO demonstrates the sensitive dependence of the ligand binding mode on ancillary ligation at the metal.

504

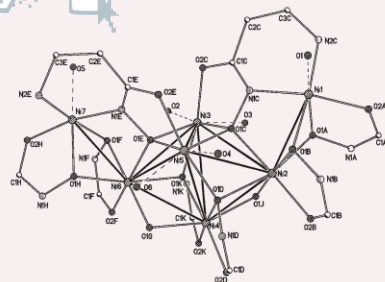
Design of bimodal mesoporous silicas with interconnected pore systems by ammonia post-hydrothermal treatment in the mild-temperature range

Zhong-Yong Yuan, Jean-Luc Blin and Bao-Lian Su



Bimodal (4 and 8 nm) mesoporous silicas with interconnected three-dimensional structure were synthesized by mild-temperature post-synthesis hydrothermal treatment of MCM-41 mesoporous materials in ammonia solution.

506

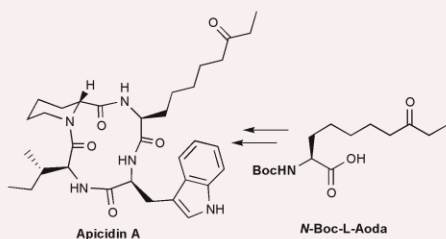


Synthesis and structure of a heptanuclear nickel(II) complex uniquely exhibiting four distinct binding modes, two of which are novel, for a hydroxamate ligand

Declan Gaynor, Zoya A. Starikova, Sergei Ostrovsky, Wolfgang Haase and Kevin B. Nolan

$[\text{Ni}_7(2\text{-dmAphaH}_{-1})_2(2\text{-dmApha})_8(\text{H}_2\text{O})_2]\text{SO}_4 \cdot 15\text{H}_2\text{O}$ which contains a trigonal bipyramidal array of nickel ions with another nickel annexed to each apex, shows both antiferromagnetic and ferromagnetic interactions and uniquely shows four distinct hydroxamate binding modes, two of which are novel.

508

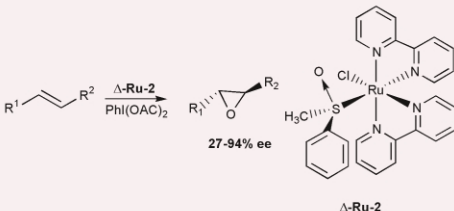


Solid-phase synthesis of apicidin A and a cyclic tetrapeptide analogue

Frédéric Berst, Mark Ladlow and Andrew B. Holmes

The solid-phase synthesis of the antiprotozoal cyclic tetrapeptide apicidin A is reported and its synthetic accessibility is contrasted with that of a structurally similar reduced cyclic tetrapeptide analogue.

510

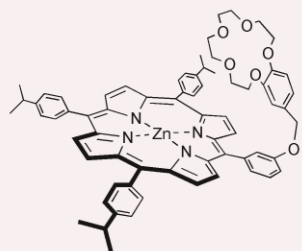


Ruthenium bis(bipyridine) sulfoxide complexes: new catalysts for alkene epoxidation

Frédéric Pezet, Hassan Ait-Haddou, Jean-Claude Daran, Isabelle Sasaki and Gilbert G. A. Balavoine

The ruthenium bis(bipyridine) sulfoxide complexes **Ru-1** and **Ru-2** exhibit high catalytic activity for epoxidation of unfunctionalized olefins in the presence of [bis(acetoxy)iodo]benzene; with the chiral catalyst, **Ru-2**, asymmetric induction up to 94% was observed for β -methylstyrene.

512

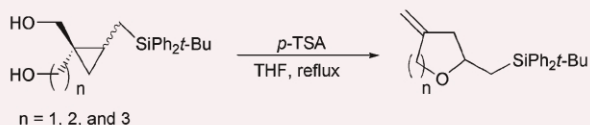


Ion pair recognition by Zn-porphyrin/crown ether conjugates: visible sensing of sodium cyanide

Yeon-Hwan Kim and Jong-In Hong

Synthesis and complexation behavior of ditopic neutral receptors composed of both a Lewis-acidic binding site (zinc porphyrin moiety) and a Lewis-basic binding site (crown ether moiety) are reported; the receptors bound only NaCN in a ditopic fashion with a color change, and in contrast other sodium salts bound to the receptors in a monotopic fashion without a color change.

514



Synthesis of γ -methylene oxacycles and α - and β -alkylidene lactones via silicon-assisted ring opening of cyclopropyl carbinols

Veejendra K. Yadav and Rengarajan Balamurugan

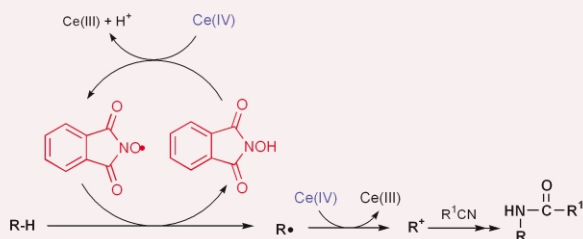
A versatile method for the synthesis of heterocycles such as 5-, 6-, and 7-membered oxacycles and 5-, and 6-membered alkylidene lactones involving silicon-assisted ring opening of cyclopropyl carbinols is described.

516

First Ritter-type reaction of alkylbenzenes using *N*-hydroxyphthalimide as a key catalyst

Satoshi Sakaguchi, Tomotaka Hirabayashi and Yasutaka Ishii

The first Ritter-type reaction of alkylbenzenes with nitriles has been successfully achieved by the use of *N*-hydroxyphthalimide (NHPI) combined with ammonium hexanitratocerate(IV) (CAN).

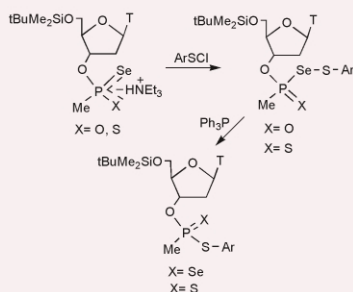


518

New examples of mixed seleno-sulfides; reactions with triphenylphosphine

Arkadiusz Chworoś, Lucyna A. Woźniak and Wojciech J. Stec

The formation of mixed seleno-sulfides by means of activation of methanephosphonoseleno(thio)ic acids with arylsulfenyl chloride is rationalized on the basis of NMR and identification of the products of their reactions with triphenylphosphine.

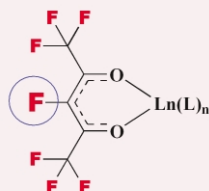


520

The first perfluoroacetylacetonate metal complexes: as unexpectedly robust as tricky to make

Viacheslav A. Petrov, William J. Marshall and Vladimir V. Grushin

The first perfluoroacetylacetonato metal complexes have been synthesized and fully characterized. There is a striking difference in hydrolytic stability of acac-F₇ before and after chelation to the metal.

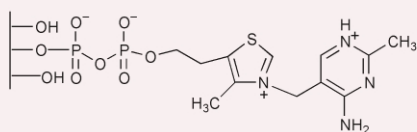


522

Practical tethering of vitamin B₁ on a silica surface *via* its phosphate group and evaluation of its activity

Ch. Vartzouma, M. Louloudi, I. S. Butler and N. Hadjiliadis

A novel synthetic approach to biomimetic materials is described, presenting attachment of vitamin B₁ on a silica surface *via* its phosphate group; evaluation of the catalytic activity of the novel material for pyruvate decarboxylation is also discussed.

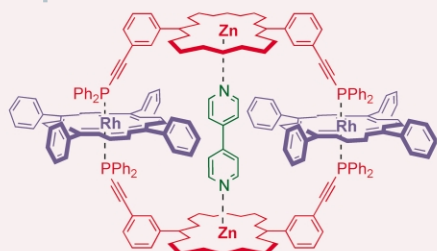


524

Amplification of a cyclic mixed-metalloporphyrin tetramer from a dynamic combinatorial library through orthogonal metal coordination

Eugen Stulz, Yiu-Fai Ng, Sonya M. Scott and Jeremy K. M. Sanders

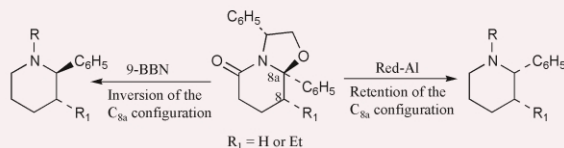
A cyclic porphyrin tetramer, consisting of two bis-phosphine substituted zinc(II) porphyrin units and two Rh(III)TPP units, is selected and amplified virtually quantitatively from a dynamic combinatorial library using 4,4'-bipy as a scaffold and using orthogonal binding modes.



526

Enantioselective synthesis of 2-arylpiperidines from chiral lactams. A concise synthesis of (–)-anabasine

Mercedes Amat, Margalida Cantó, Núria Llor and Joan Bosch

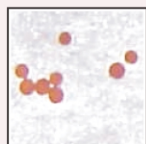
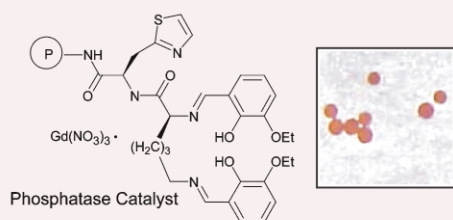


The enantiodivergent synthesis of 2-arylpiperidines and the diastereodivergent synthesis of *cis*- and *trans*-3-alkyl-2-arylpiperidines from (*R*)-phenylglycinol-derived bicyclic lactams is reported.

528

Discovery of a novel synthetic phosphatase from a bead-bound combinatorial library

Shelley C. Danek, Jerome Queffelec and James P. Morken

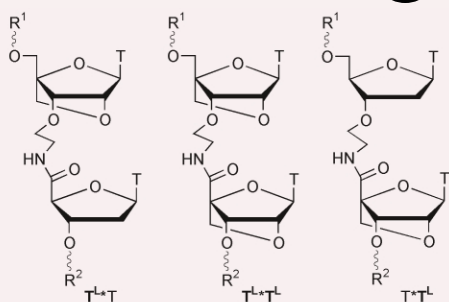


Using split/pool encoded synthesis and a colorimetric catalysis assay, a number of synthetic phosphatase catalysts were developed.

530

Oligodeoxynucleotides containing amide-linked LNA-type dinucleotides: synthesis and high-affinity nucleic acid hybridization

Anne Lauritsen and Jesper Wengel

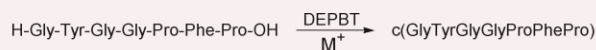
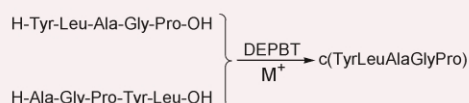


A destabilizing non-natural amide internucleoside linkage has been converted into a strongly stabilizing one by exchanging a DNA monomer with an LNA-type monomer.

532

Promotion of cyclization of linear pentapeptides and heptapeptide by different univalent metal ions

Yun-hua Ye, Mian Liu, Yan-chun Tang and Xiaohui Jiang

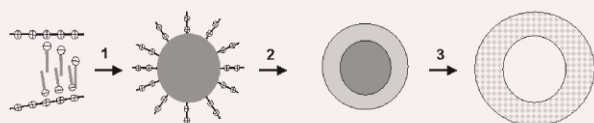


Univalent metal ions such as Na^+ , K^+ and Cs^+ can enhance not only the cyclization yields of some linear pentapeptides and heptapeptide but also their cyclization rates.

534

Hollow nanoparticles via stepwise complexation and selective decomplexation of poly(ethylene imine)

Sascha General, Jan Rudloff and Andreas F. Thünemann

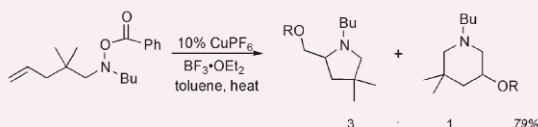


The preparation of hollow nanoparticles with amino groups on the inner side via the stepwise complexation and selective decomplexation of poly(ethylene imine) is presented.

536

Copper(I) catalysed cyclisation of unsaturated *N*-benzyloxyamines: an aminohydroxylation *via* radicals

Michael Noack and Richard Göttlich

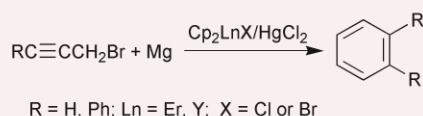


The Sharpless aminohydroxylation is not the only way to synthesise aminoalcohols from alkenes, but the described copper(I)-catalysed radical reaction leads to aminohydroxylation too.

538

Novel Cp₂LnX-mediated coupling–cyclization of propargyl bromide: a new construction of the benzene ring skeleton

Ruyi Ruan, Jie Zhang, Xigeng Zhou and Ruifang Cai

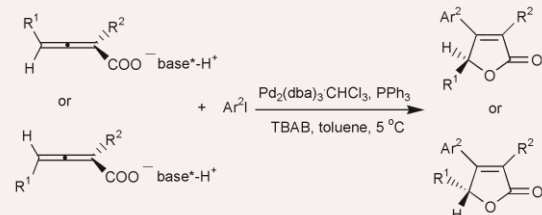


A novel Cp₂LnX-mediated coupling–cyclization of propargyl bromide is described which provides a new method for the construction of the benzene ring skeleton.

540

Mechanistic switch leading to highly efficient chirality transfer in Pd(0)-catalyzed coupling–cyclization of aryl iodides with 1 : 1 acid–base salts of 2,3-allenoic acids and L-(–)-cinchonidine or D-(+)-/L-(–)-α-methylbenzylamine. Enantioselective synthesis of highly optically active 3-aryl polysubstituted butenolides

Shengming Ma and Zhangjie Shi

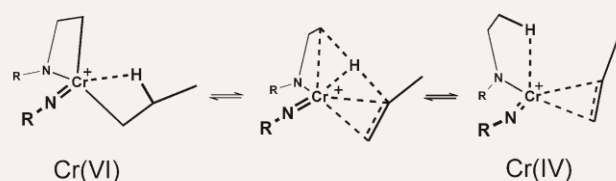


Highly optically active polysubstituted butenolides were prepared from aryl halides and 1 : 1 salts of optically active 2,3-allenoic acid–base *via* oxidative addition–coordinative cyclization–reductive elimination.

542

Reduction of chromium in ethylene polymerisation using bis(imido)chromium(VI) catalyst precursors

Vidar R. Jensen and Knut J. Børve

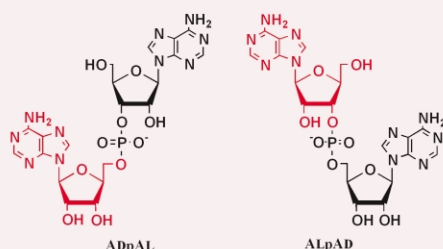


Hybrid density functional calculations on ethylene complexes of bis(imido)chromium(VI) alkyls have revealed a facile reductive elimination reaction, suggesting that the active species in ethylene polymerisation using bis(imido)chromium(VI) precursors involves chromium in oxidation state IV or lower.

544

Helical structure of heterochiral RNA dimers: helical sense of ApA is determined by chirality of 3'-end residue

Hidehito Urata, Makiko Go, Norihiko Ohmoto, Katsuhiko Minoura and Masao Akagi



The helical structures of heterochiral ApAs have shown that the chirality of the 3'-end residue is the primary factor for determining the helical sense of ApA.

COPIES OF CITED ARTICLES

The Library and Information Centre (LIC) of the RSC offers a first class Document Delivery Service for items in Chemistry and related subjects. Contact the LIC, The Royal Society of Chemistry, Burlington House, Piccadilly, London W1V 0BN, UK.

This service is only available from the LIC in London and not the RSC in Cambridge.

Contents lists in advance of publication are available on the web via www.rsc.org/chemcomm – or take advantage of our free e-mail alerting service (www.rsc.org/ej_alert) to receive notification each time a new list becomes available.



Supplementary crystallographic data are available: see article for further information.



Electronic supplementary information is available on <http://www.rsc.org/esi>: see article for further information.

- Adams, Harry, 418
 Addison, Anthony W., 468
 Ait-Haddou, Hassan, 510
 Akagi, Masao, 544
 Akutagawa, Tomoyuki, 408
 Alonso, Jorge, 426
 Amat, Mercedes, 526
 Anand, Venkataramanarao G., 462
 Anilkumar, Gopinathan, 450
 Araki, Hiromi, 402
 Balamurugan, Rengarajan, 514
 Balavoine, Gilbert G. A., 510
 Beauchemin, André, 466
 Bélanger-Gariépy, Francine, 466
 Bell, Stephen G., 490
 Berst, Frédéric, 508
 Bibal, Brigitte, 432
 Blin, Jean-Luc, 504
 Boldog, Iштvan, 436
 Børve, Knut J., 542
 Bosch, Joan, 526
 Boyd, Alan S. F., 464
 Boyd, Helen D., 490
 Butcher, Raymond J., 468
 Butler, I. S., 522
 Cai, Ruifang, 538
 Campbell, Sophie, 490
 Cantó, Margalida, 526
 Chandrashekar, Tavarekere K., 462
 Chang, Ramsay, 452
 Charette, André, 466
 Chernega, Alexander N., 436
 Chworos, Arkadiusz, 518
 Clunas, Scott, 418
 Cole, Adam P., 502
 Coppel, Yannick, 414
 Coppens, Philip, 424
 Cullis, Paul M., 458
 D'Acquarica, Ilaria, 474
 Danek, Shelley C., 528
 Danopoulos, Andreas A., 482
 Daran, Jean-Claude, 510
 Daub, Joerg, 460
 Davis, Jason J., 393
 Declercq, Jean-Paul, 432
 Dell'Anna, Maria Michela, 434
 Desiderio, Paola, 474
 Di Tullio, Alessandra, 474
 Diemann, Ekkehard, 440
 Domasevitch, Konstantin V., 436
 Dutasta, Jean-Pierre, 432
 Eichen, Yoav, 404
 Ellis, David, 464
 Enders, Dieter, 498
 Enright, Gary D., 466
 Farwell, James D., 456
 Fearnley, Stephen Philip, 438
 Fenton, David E., 418
 Fernández, Rosario, 498
 Francoeur, Sébastien, 466
 Franke, Dirk, 494
 Fröba, Michael, 406
 Fu, Yu, 480
 Fujishima, Akira, 486
 Fukazawa, Yoshimasa, 402
 Funabiki, Takuzo, 412
 Furuike, Tetsuya, 430
 Furusawa, Hiroyuki, 470
 Gallo, Vito, 434
 Gasparini, Francesco, 474
 Gaynor, Declan, 506
 Gelbrich, Thomas, 482
 General, Sascha, 534
 Giannessi, Fabio, 474
 Giles, Barry T., 464
 Go, Makiko, 544
 Goldston, Jr., Harold M., 416
 Göttlich, Richard, 536
 Grushin, Vladimir V., 520
 Haase, Wolfgang, 506
 Hadjiliadis, N., 522
 Haino, Takeharu, 402
 Hamamoto, Hiromi, 450
 Han, Sang Woo, 442
 Hanabusa, Kenji, 428
 Harger, Martin J. P., 458
 Hasegawa, Tatsuo, 408
 Hecker, Walburga, 500
 Hill, H. Allen O., 393
 Hirabayashi, Tomotaka, 516
 Hiratani, Kazuhisa, 420
 Hitchcock, Peter B., 456
 Hitomi, Yutaka, 412
 Hoffmann, Nils, 454
 Holmes, Andrew B., 508
 Hong, Jong-In, 512
 Houjou, Hirohiko, 420
 Hu, Ai-Guo, 480
 Huang, Kuo-Wei, 502
 Huang, R. B., 472
 Hursthouse, Michael B., 482
 Huy, Ngoc Hoa Tran, 454
 Inoue, Masaaki, 428
 Inui, Nobuhiko, 412
 Ishii, Yasutaka, 516
 Izaki, Masanobu, 476
 Jarowicki, Krzysztof, 426
 Jensen, Vidar R., 542
 Jereb, Marjan, 488
 Jiang, Xiaohui, 532
 Jones, Peter G., 454
 Kapon, Moshe, 404
 Kato, Takashi, 428
 Kim, Kwan, 442
 Kim, Yeon-Hwan, 512
 Kita, Yasuyuki, 450
 Kocienski, Philip J., 426
 Kolotilov, Sergey V., 468
 Komarchuk, Vasilij V., 436
 Kuhlmann, Christoph, 440
 Ladlow, Mark, 508
 Lappert, Michael F., 456
 Lassaletta, José M., 498
 Lauritsen, Anne, 530
 Lee, Joowook, 486
 Lee, Seung Joon, 442
 Leitner, Walter, 410
 Letzel, Matthias C., 440
 Liang, Yingqiu, 492
 Liu, Mian, 532
 Llor, Núria, 526
 Long, L. S., 472
 Long, Richard Q., 452
 Lorbach, Volker, 494
 Louloudi, M., 522
 Luo, Xuzhong, 492
 Ma, Bao-Qing, 424
 Ma, Shengming, 540
 Macgregor, Stuart A., 464
 Maeda, Matsutaka, 412
 Mahanthappa, Mahesh K., 502
 Market, Eleonora, 438
 Marshall, William J., 520
 Mastroilli, Piero, 434
 Masuda, Toshio, 478
 Mathey, François, 454
 Matsuno, Hisao, 470
 Meunier, Bernard, 414
 Milne, Jacqueline E., 426
 Minoura, Katsuhiko, 544
 Mizoshita, Norihiro, 428
 Monde, Kenji, 430
 Monobe, Hirosato, 428
 Morken, James P., 528
 Muck, Sandra, 474
 Müller, Achim, 440
 Müller, Michael, 494
 Nakamura, Takayoshi, 408
 Ng, Yiu-Fai, 524
 Nicholas, Kenneth M., 484
 Nieger, Martin, 494
 Nieuwenhuysen, Mark, 444
 Niikura, Kenichi, 430
 Nishihara, Sadafumi, 408
 Nishimura, Shin-Ichiro, 430
 Noack, Michael, 536
 Nobile, Cosimo Francesco, 434
 Nolan, Kevin B., 506
 Nomura, Ryoji, 478
 Ohmoto, Norihiko, 544
 Okahata, Yoshio, 470
 Opallo, Marcin, 448
 Orton, Erica L., 490
 Osborne, Daire, 444
 Ostrovsky, Sergei, 506
 Park, Su-Moon, 486
 Parmar, Virinder S., 500
 Pavlishchuk, Vitaly V., 468
 Penoni, Andrea, 484
 Petrov, Viacheslav A., 520
 Pezet, Frédéric, 510
 Piccirilli, Fabrizio, 474
 Pillai, Unnikrishnan R., 422
 Pinto, Mauricio R., 446
 Ponomarova, Vira V., 436
 Prasad, Ashok K., 500
 Prieto, Auxiliadora, 498
 Prushan, Michael J., 468
 Pushpan, Simi K., 462
 Queffelec, Jerome, 528
 Rao, Maddali L. N., 420
 Riddle, Austin D., 490
 Robert, Anne, 414
 Romanazzi, Giuseppe, 434
 Rosair, Georgina M., 464
 Ruan, Ruyi, 538
 Rudloff, Jan, 534
 Saczek-Maj, Monika, 448
 Sahle-Demessie, Endalkachew, 422
 Sakaguchi, Satoshi, 516
 Sanders, Jeremy K. M., 524
 Sankar, Jeyaraman, 462
 Sasaki, Isabelle, 510
 Schanze, Kirk S., 446
 Scott, Sonya M., 524
 Scribner, Alicia N., 416
 Seitz, Oliver, 500
 Shah, S. Qaiser Nazir, 440
 Shen, Zhen, 460
 Shi, Zhangjie, 540
 Shimizu, Yo, 428
 Shterenberg, Alexander, 404
 Sieler, Joachim, 436
 Singh, Ishwar, 500
 Starikova, Zoya A., 506
 Stavber, Stojan, 488
 Stec, Wojciech J., 518
 Steinke, Joachim H. G., 496
 Stevenson, Julie-Anne, 490
 Stevenson, Paul J., 444
 Strauss, Joerg, 460
 Streubel, Rainer, 454
 Stulz, Eugen, 524
 Su, Bao-Lian, 504
 Sugio, Daisuke, 412
 Sukegawa, Takeshi, 430
 Suranna, Gian Paolo, 434
 Suwinska, Kinga, 404
 Tan, Chunyan, 446
 Tang, Yan-chun, 532
 Tender, Leonard M., 416
 Theysen, Nils, 410
 Thompson, Laurence K., 468
 Thünemann, Andreas F., 534
 Tiemann, Michael, 406
 Tinant, Bernard, 432
 Tinti, Maria Ornella, 474
 Tohma, Hirofumi, 450
 Tooze, Robert P., 482
 Trammell, Scott A., 416
 Tryk, Donald A., 486
 Tuncel, Dönüs, 496
 Turner, Boaz, 404
 Ukon, Masakatsu, 428
 Urata, Hidehito, 544
 Vartzouma, Ch., 522
 Vázquez, Juan, 498
 Venkatraman, Sundararaman, 462
 Villani, Claudio, 474
 Wang, Li-Xin, 480
 Watanabe, Tsuyoshi, 428
 Waymouth, Robert M., 502
 Welch, Alan J., 464
 Wengel, Jesper, 530
 Wilson, Neil M. M., 464
 Winston, Scott, 482
 Wismach, Cathleen, 454
 Wong, Luet-Lok, 490
 Wozniak, Lucyna A., 518
 Wu, Sanxie, 492
 Xie, Jian-Hua, 480
 Yadav, Veejendra K., 514
 Yamada, Katsuhiko, 478
 Yamagishi, Akihiko, 430
 Yamanaka, Yuko, 402
 Yang, Ralph T., 452
 Yang, S. Y., 472
 Ye, Yun-hua, 532
 Yen, Zhong-Yong, 504
 Zhang, Jie, 538
 Zheng, L. S., 472
 Zhou, Hai, 480
 Zhou, Qi-Lin, 480
 Zhou, Xigeng, 538
 Zupan, Marko, 488